

**DNA and Chromosomes:
E2F1 Localizes to Sites of UV-induced DNA
Damage to Enhance Nucleotide Excision
Repair**

DNA AND
CHROMOSOMES



Ruifeng Guo, Jie Chen, Feng Zhu, Anup K.
Biswas, Thomas R. Berton, David L. Mitchell
and David G. Johnson

J. Biol. Chem. 2010, 285:19308-19315.

doi: 10.1074/jbc.M110.121939 originally published online April 22, 2010

Access the most updated version of this article at doi: [10.1074/jbc.M110.121939](https://doi.org/10.1074/jbc.M110.121939)

Find articles, minireviews, Reflections and Classics on similar topics on the [JBC Affinity Sites](https://www.jbc.org/).

Alerts:

- [When this article is cited](#)
- [When a correction for this article is posted](#)

[Click here](#) to choose from all of JBC's e-mail alerts

Supplemental material:

<http://www.jbc.org/content/suppl/2010/04/22/M110.121939.DC1.html>

This article cites 44 references, 25 of which can be accessed free at
<http://www.jbc.org/content/285/25/19308.full.html#ref-list-1>

E2F1 Localizes to Sites of UV-induced DNA Damage to Enhance Nucleotide Excision Repair*[§]

Received for publication, March 9, 2010, and in revised form, April 21, 2010. Published, JBC Papers in Press, April 22, 2010, DOI 10.1074/jbc.M110.121939

Ruifeng Guo^{‡§}, Jie Chen^{‡§}, Feng Zhu[‡], Anup K. Biswas[‡], Thomas R. Berton[‡], David L. Mitchell^{‡§}, and David G. Johnson^{‡§1}

From the [‡]Department of Carcinogenesis, University of Texas M. D. Anderson Cancer Center, Science Park Research Division, Smithville, Texas 78957 and the [§]University of Texas Graduate School of Biomedical Sciences at Houston, Houston, Texas 77030

The E2F1 transcription factor is a well known regulator of cell proliferation and apoptosis, but its role in the DNA damage response is less clear. Using a local UV irradiation technique and immunofluorescence staining, E2F1 is shown to accumulate at sites of DNA damage. Localization of E2F1 to UV-damaged DNA requires the ATM and Rad3-related (ATR) kinase and serine 31 of E2F1 but not an intact DNA binding domain. E2F1 deficiency does not appear to affect the expression of nucleotide excision repair (NER) factors, such as XPC and XPA. However, E2F1 depletion does impair the recruitment of NER factors to sites of damage and reduces the efficiency of DNA repair. E2F1 mutants unable to bind DNA or activate transcription retain the ability to stimulate NER. These findings demonstrate that E2F1 has a direct, non-transcriptional role in DNA repair involving increased recruitment of NER factors to sites of damage.

UV radiation causes several forms of DNA damage, the most prominent of these being the cyclobutane pyrimidine dimer (CPD)² and 6–4 pyrimidine-pyrimidone photoproduct ((6–4)PP). This damage is repaired by the NER pathway, which can be further partitioned into global genome NER (GG-NER) and transcription-coupled repair. Transcription-coupled NER repairs damage in actively transcribed DNA strands, whereas GG-NER is used to repair the majority of damage throughout the genome (1). The importance of NER is illustrated by the hereditary syndrome xeroderma pigmentosum (XP), which is caused by mutations in one of several NER genes and characterized by hypersensitivity to sunlight and a strong predisposition to skin cancer.

* This work was supported, in whole or in part, by National Institutes of Health Grants CA016672 and CA079648 (to D. G. J.), K01-CA106603 (to T. R. B.) and CA105345, ES007784, and ES007247 through the M. D. Anderson Cancer Center. This research was performed in partial fulfillment of the requirements for the Ph.D. degree from The University of Texas Graduate School of Biomedical Sciences at Houston; University of Texas M. D. Anderson Cancer Center, Houston, TX.

[§] The on-line version of this article (available at <http://www.jbc.org>) contains supplemental Figs. S1 and S2.

¹ To whom correspondence should be addressed: P. O. Box 389, Smithville, TX 78957. Tel.: 512-237-9511; Fax: 512-237-6533; E-mail: djohnson@mdanderson.org.

² The abbreviations used are: CPD, cyclobutane pyrimidine dimer; (6–4)PP, 6–4 pyrimidine-pyrimidone photoproduct; NER, nucleotide excision repair; GG-NER, global genome NER; XP, xeroderma pigmentosum; ATR, ATM and Rad3-related kinase; TopBP1, topoisomerase II-binding protein 1; ATM, ataxia telangiectasia-mutated kinase; DSB, double strand break; NHF, normal human fibroblast; AT, ataxia-telangiectasia; DAPI, 4',6-diamidino-2-phenylindole; CMV, cytomegalovirus; siRNA, small interference RNA; GFP, green fluorescent protein.

The ATR kinase plays a major role in the DNA damage response initiated by UV radiation. Recent studies have shown that single-stranded DNA, which occurs at stalled replication or transcription forks or during the process of NER, constitutes the signal for ATR activation (2–4). ATR is recruited to sites of single-stranded DNA through its association with ATR-interacting protein, which in turn binds to the single-stranded DNA-binding protein replication protein A (4). ATR is then activated through a physical interaction with topoisomerase II-binding protein 1 (TopBP1), which is independently recruited to sites of damage through an interaction with the Rad9-Rad1-Hus1 (9-1-1) complex (5, 6). Once active, ATR phosphorylates substrates such as Claspin, Chk1, and p53 to promote repair, establish cell cycle checkpoints, or induce apoptosis.

ATR and the related ataxia telangiectasia-mutated (ATM) kinase also phosphorylate the E2F1 transcription factor on serine 31, a site not conserved in other E2F family members (7). E2Fs regulate the expression of numerous genes involved in cell cycle progression and apoptosis and are key determinants of cell fate (8). Phosphorylation of E2F1 on serine 31 stimulates binding to 14-3-3 τ , which leads to E2F1 stabilization following DNA damage (9). Serine 31 phosphorylation also creates a binding site for one of the eight BRCA1 C-terminal domains of TopBP1 (10). TopBP1 binding to E2F1 inhibits the transcriptional activity of E2F1 independent of the retinoblastoma tumor suppressor. In addition, TopBP1 binding results in the accumulation of E2F1 at sites of DNA double-strand breaks (DSBs) (10).

In response to agents that cause DSBs, E2F1 stabilization contributes to the induction of apoptosis by transcriptionally activating *p73* and perhaps other pro-apoptotic target genes (11, 12). In response to UV, however, E2F1 does not transcriptionally activate *p73* or promote apoptosis (12). In fact, we have previously shown that E2F1 has an anti-apoptotic function in response to UV radiation (13, 14). Mice lacking E2F1 had higher levels of apoptosis in their epidermis following UV irradiation compared with wild-type mice while transgenic mice overexpressing E2F1 had reduced levels of UV-induced apoptosis. E2F1-mediated survival in response to UV correlated with an effect on DNA repair, which was impaired in the absence of E2F1 and stimulated by E2F1 overexpression (13). Here we provide evidence that E2F1 enhances GG-NER through a novel mechanism that is independent of its function as a transcriptional regulator.

EXPERIMENTAL PROCEDURES

Cells—Primary dermal normal human fibroblasts (NHF, GM08399), SV40-transformed dermal fibroblasts (GM00637),

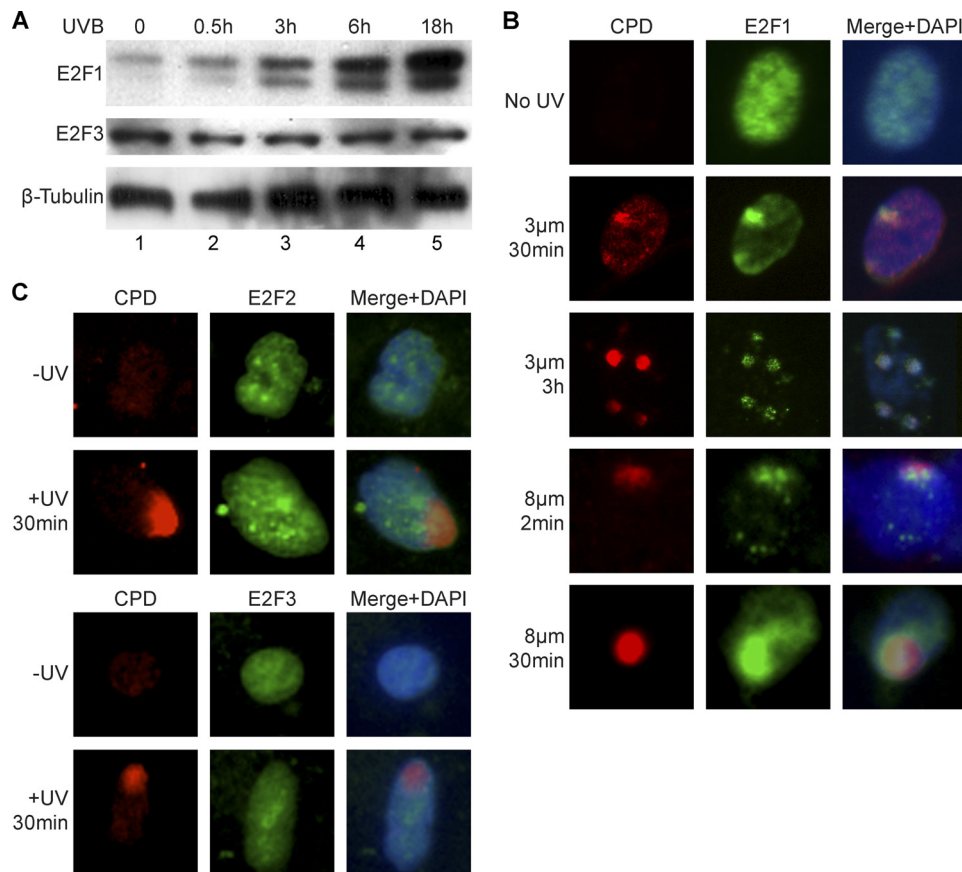


FIGURE 1. E2F1 accumulates at sites of UV-induced DNA damage. *A*, primary NHFs were irradiated with 500 J/m² of UVB or mock treated (*lane 1*) and harvested at the indicated times post-irradiation. Western blot analysis was performed on whole cell extracts using antibodies specific for E2F1, E2F3, or β -tubulin. *B*, NHFs were untreated or locally irradiated with 50 or 100 J/m² of UVC through polycarbonate filters with pores of 3 or 8 μ m as indicated. 2 min, 30 min, or 3 h post-irradiation, cells were fixed and stained for CPD (red) and E2F1 (green) by indirect immunofluorescence. Cells were counterstained with DAPI to show nuclei and images were digitally recorded. *C*, NHFs were untreated or locally irradiated with 50 J/m² of UVC and stained for CPD and E2F2 or E2F3 as described above.

and primary fibroblasts from ataxia-telangiectasia (AT, GM02052) and Seckel syndrome (ATR-deficient, GM18366) patients were obtained from Coriell Institute. HeLa and HCT116 cells were obtained from ATCC. All cells were maintained in Dulbecco's modified Eagle's medium (HyClone) supplemented with 10% fetal bovine serum (Atlanta) except HCT116 cells, which were maintained in McCoy's 5A Medium (Invitrogen) with 10% fetal bovine serum.

UV Treatment—For general UV treatment, UVB was delivered by Westinghouse FS20 sunlamps filtered through cellulose acetate (Kodacel from Kodak, St. Louis, MO) with a wavelength cutoff of 290 nm. Dosimetry was determined with a IL1400 photometer coupled to a SCS 280 probe (International Light, Newburyport, MA). Because filters absorb ~90% of the UV radiation (15), it was necessary to use UVC for the co-localization assays, because UVC is more efficient at inducing DNA damage compared with the more physiological relevant UVB radiation. UVC was delivered by Phillips Sterilamp G8T5 bulbs emitting predominantly 254 nm. The dose was measured using an IL-1400A Photometer coupled to SEL 240 detector.

Western Blot and Co-immunoprecipitation—Cells were mock treated or treated with 500 J/m² of UVB, and whole cell lysates were obtained using 1 \times lysis buffer (Cell signaling).

E2F1 antibody-conjugated Protein A/G-agarose (Santa Cruz Biotechnology, Santa Cruz, CA) was used for immunoprecipitation, and the precipitate was analyzed by Western blot using E2F1 or TopBP1 antibodies. Antibodies/antisera were obtained from the following sources: E2F1 (C-20 and KH95), β -tubulin, E2F2, E2F3, and p62, Santa Cruz Biotechnology; CPD and (6–4)PP, MBL; XPA polyclonal, Santa Cruz Biotechnology; XPA monoclonal (12F5), Lab Vision; and TopBP1, Bethyl Laboratories. Rabbit polyclonal antisera to the CPD and (6–4)PP photoproducts were developed by Dr. David Mitchell.

Filtered UV Irradiation/Immunofluorescence Assay—Co-localization of proteins with UV-induced DNA damage was performed as previously described (15–17). Briefly, cells grown on chamber slides (Nunc) were rinsed in phosphate-buffered saline leaving a thin layer of buffer on top. Sterile isopore polycarbonate membrane filter (Mili-pore) containing pores of either 3 or 8 μ m in diameter were placed on top of the cells, and the slides were irradiated from above with UVC. The filter was then removed, and cells were incubated for designated time points before a cytoskeleton

extraction procedure. After washing, cells were fixed in phosphate-buffered saline containing 2% formaldehyde and 0.2% Triton X-100. For immunofluorescent staining, fixed cells were incubated with 3% bovine serum albumin, washed, and treated with 2 M HCl for 5 min at 37 $^{\circ}$ C to denature the DNA. Washed cells were then incubated with appropriate primary antibodies (e.g. specific for CPD and E2F1) followed by incubation with appropriate fluorescent secondary antibodies (Alexa 488 or Alexa 594, Invitrogen). Cells were then stained with DAPI and sealed in mounting media (Vector Laboratory) with coverslips. The images were captured, digitally recorded, and analyzed using a Nikon eclipse 80i microscope equipped with an X-cite 120 fluorescence illumination system and Metamorph image analysis software. Percent co-localization was determined by scoring 100 randomly selected cells for each experimental group as previously described (15, 17).

Chromatin Immunoprecipitation-coupled UV-induced DNA Damage Detection Assay—This assay was performed as previously reported (18) with minor modifications. Briefly, cells were mock treated or treated with 500 J/m² of UVB, then fixed with 1% formaldehyde for 15 min at room temperature. Fixed cells were harvested by standard cell lysis buffer and sonicated to shear the DNA. Immunoprecipitations were performed with

E2F1 Directly Enhances NER

antibodies against E2F1 or E2F2, and the precipitated DNA was reverse cross-linked and purified. After quantification of the DNA, the amount of UV-induced DNA damage pulled down by the binding proteins was detected by a slot-blot assay. As a control, the same DNA samples were also amplified by PCR for the proliferating cell nuclear antigen promoter, which is both an E2F1 and E2F2 transcriptional target.

Slot-blot DNA Repair Assay—UV-induced DNA damage was detected as described (19) with minor modifications. Briefly, cells were treated with 500 J/m² of UVB and incubated for the designated time periods before isolating genomic DNA using the GenElute kit (Sigma). DNA was quantified, and 0.5 μg of DNA was spotted onto nitrocellulose membranes (Genemate) using a slot-blot transfer apparatus (Bio-Rad). The UV-induced DNA damage was detected by an immunoblot procedure using antibodies against (6–4)PP (1:1000) and CPD (1:2000). The membrane was re-probed with antibody against single-stranded DNA (Chemicon, MAB3034) for loading control. The densities of the bands were quantified by using ImageJ, and the graphs were plotted accordingly after normalization with the loading control.

Plasmids and Small Interference RNA—The cDNAs of human *E2F1*, including the wild-type, serine S31A mutant, DNA binding domain mutant (E138), DP dimerization domain deletion mutant (Δ206–220), Marked box domain deletion mutant (Δ283–358), and C terminus deletion mutant (Δ375–437), were inserted into a p3XFLAG CMV vector (Sigma) at the HindIII/XbaI sites. The cDNAs of wild-type E2F1 and S31A mutant were also inserted into a pEGFP-C1 vector (Clontech) to generate the green fluorescence protein fused to E2F1. Small interference RNAs (siRNAs) against the human *E2F1* coding region (E2F-1 siRNA sc29297: strand 5169, CACCUGAUGAAUAUCUGUA; strand 5170, CCUGAUGAAUAUCUGUACU; and strand 5171, GAGUCUGUGUGGUGUGUAU) and 3'-untranslated region (E2F1 siRNA sc29297 strand 5171 GAGUCUGUGUGGUGUGUAU and E2F1 siRNA sc44258 strand 16661 GCUUUAUGGAGCGUUAUU) were purchased from Santa Cruz Biotechnology. Transfections were performed with either Oligofectamine (for primary normal human fibroblasts) or Lipofectamine 2000 reagent (Invitrogen) following the manufacturer's recommended protocol. Because of differences in the steady-state expression levels of the various FLAG-E2F1 mutant proteins, the amounts of each plasmid transfected into cells for the rescue experiments were adjusted as follows: wild type, 2 μg; S31A, 8 μg; E138, 0.5 μg; Δ206–220, 2 μg; Δ283–358, 1 μg; and Δ375–437, 0.5 μg.

RESULTS

E2F1 Accumulates at Sites of UV-induced DNA Damage—Among the E2F family, E2F1 is specifically stabilized in response to several types of DNA damage (20–22), and we confirmed this finding in NHF cells following UVB irradiation (Fig. 1A). In some settings, E2F1 stabilization in response to DNA damage contributes to the induction of apoptosis (7, 23). However, we found that mice lacking E2F1 are hypersensitive to UV-induced apoptosis, whereas transgenic expression of E2F1 can suppress apoptosis in response to UV (13, 14). We also found that the inactivation of *E2f1* in mice impairs GG-NER

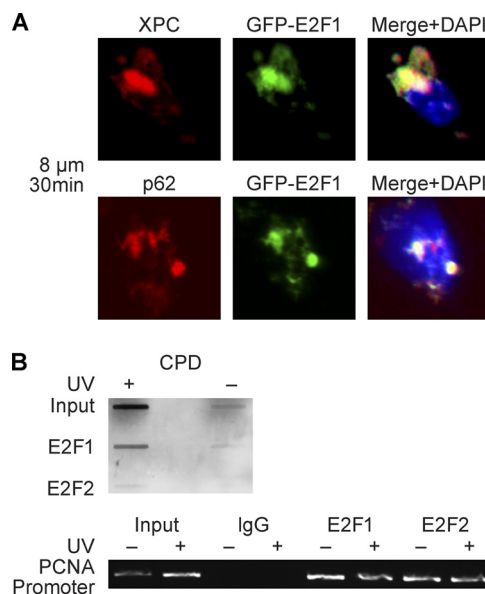


FIGURE 2. E2F1 co-localizes with NER factors and associates with damaged DNA. A, HeLa cells were transfected with plasmids expressing wild-type E2F1 fused to enhanced GFP. 24 h post-transfection, cells were exposed to 50 J/m² of UVC through an 8-μm pore filter and stained 30 min later for XPC or p62 (red). Slides were counterstained with DAPI, and images were digitally recorded as previously described. B, NHFs were mock treated or exposed to 500 J/m² of UVB and fixed with 1% formaldehyde for 15 min. Cells were lysed in the standard lysis buffer and chromatin immunoprecipitation was performed using antibody to either E2F1 or E2F2. The DNA in the precipitates was purified and analyzed by slot blotting for CPD photoproducts (top) or by PCR for the *PCNA* promoter region (bottom).

and suggested the anti-apoptotic and pro-survival function of E2F1 following UV treatment might be related to this ability to enhance DNA repair (13).

Given that E2F1 is recruited to sites of DSBs (10), we examined whether E2F1 might also localize to sites of UV-induced DNA damage using the filtered UV irradiation-coupled immunofluorescence method (15–17). In this assay, cells are irradiated with UV through a filter and subnuclear regions containing DNA damage are identified using an antibody specific for the CPD DNA photoproduct. Because the filter absorbs most of the radiation, it was necessary to use UVC for these co-localization experiments, because UVC is more efficient than UVB at inducing DNA damage. E2F1 was found to rapidly accumulate at sites of UV-induced DNA damage, before significant E2F1 stabilization, and to remain co-localized with CPD at least 3 h post-irradiation (Fig. 1B). In contrast, the E2F2 and E2F3 proteins did not co-localize with sites of DNA damage after the same filtered UV treatment (Fig. 1C). An E2F1 construct fused to green fluorescence protein (GFP) was also found to co-localize with NER factors XPC and p62 after UV irradiation (Fig. 2A). To further confirm our finding that E2F1 associates with damaged DNA, we employed a chromatin immunoprecipitation assay and found that E2F1 could specifically pull down DNA fragments containing UV-induced damage (Fig. 2B). In contrast, E2F2 did not associate with damaged DNA but did associate with an E2F transcriptional target, the *PCNA* promoter, as efficiently as E2F1.

ATR and E2F1 Serine 31 Are Important for the Accumulation of E2F1 at Sites of UV Damage—E2F1 is phosphorylated at serine 31 by the ATM and ATR kinases in response to DNA dam-

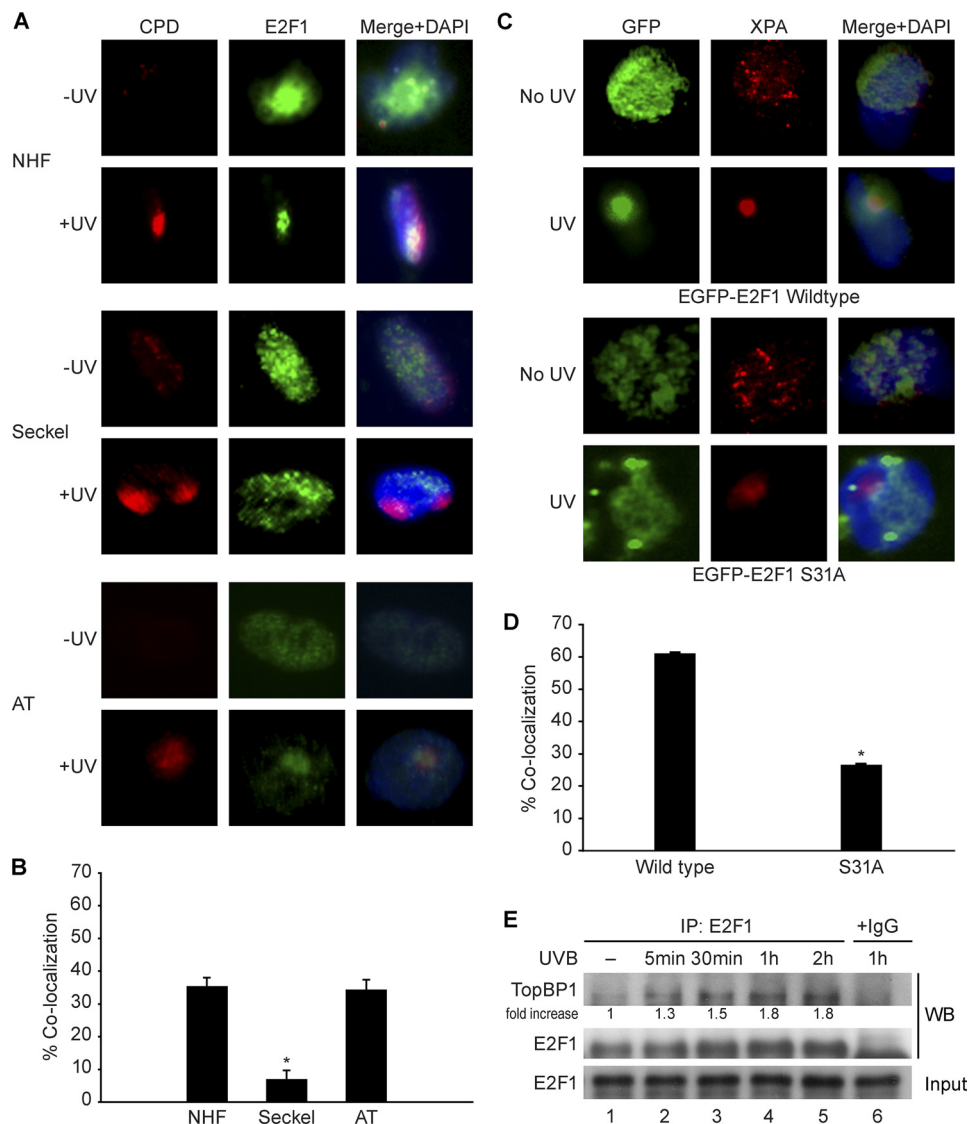


FIGURE 3. ATR and E2F1 serine 31 are required for the accumulation of E2F1 at sites of UV damage. *A*, primary NHFs, ATR-deficient human fibroblasts from a Seckel Syndrome patient (Seckel cells), and ATM-deficient human fibroblasts from an ataxia-telangiectasia patient (AT cells) were mock treated or exposed to 50 J/m^2 of UVC through an $8\text{-}\mu\text{m}$ pore filter. 30 min post-irradiation, cells were fluorescently stained for CPD (red) and E2F1 (green) and counterstained with DAPI. *B*, 100 randomly selected cells were scored for co-localization of CPD and E2F1 in each of the cell types indicated. The average of three independent experiments is presented. *, indicates statistically significant difference from NHFs by Student's *t* test ($p < 0.05$). *C*, HeLa cells were transfected with plasmids expressing GFP fused to either wild-type E2F1 or E2F1 mutated at serine 31 (S31A). 24 h post-transfection, cells were exposed to 50 J/m^2 of UVC through an $8\text{-}\mu\text{m}$ pore filter and 30 min later stained for XPA (red). Slides were then counterstained with DAPI, and images were digitally recorded as above. *D*, co-localization of XPA and GFP shown in *C* were scored and plotted as described above. The average of two independent experiments is presented. *, statistically significant difference ($p < 0.05$). *E*, HEK293 cells were untreated (lane 1) or exposed to 500 J/m^2 of UVB and harvested at different time points post-exposure (lanes 2–5) as indicated. Co-immunoprecipitation was performed using antibody to E2F1 (Santa Cruz Biotechnology, KH95) (lanes 1–5) and normal mouse IgG as negative control (lane 6). The precipitate was subjected to Western blot analysis for TopBP1 (top panel) and E2F1 (middle panel). The input for E2F1 is shown by Western blot (lower panel). The -fold increase in TopBP1 association was calculated by determining the density of the TopBP1 band and normalizing to the intensity of the E2F1 input band.

age (7). This phosphorylation event is involved in E2F1 stabilization and its localization to sites of DSBs (9, 10). To determine the role of the ATM and ATR kinases in regulating the response of E2F1 to UV, we examined the co-localization of E2F1 with CPD in NHFs, ATM-deficient human fibroblasts (AT cells), or ATR-deficient Seckel Syndrome fibroblasts. We observed that the localization of E2F1 was significantly decreased by 4-fold in

ATR-deficient cells, but not affected in the ATM-deficient cells when compared with NHFs (Figs. 3, *A* and *B*). To determine the role of serine 31 in E2F1 localization, plasmids expressing GFP fused to either wild-type or serine 31 (S31A) mutated E2F1 were transfected into HeLa cells followed by filtered UV treatment and immunostaining. Compared with wild-type E2F1, the S31A mutant showed a significantly reduced ability to accumulate at sites of UV damage as indicated by decreased co-localization with the NER protein XPA (Fig. 3, *C* and *D*). Taken together, these findings indicate that the ATR-mediated phosphorylation of E2F1 at serine 31 is important for the efficient localization of E2F1 to sites of UV damage.

Phosphorylation of E2F1 at serine 31 creates a binding site for one of the BRCA1 C-terminal domains of TopBP1, and this interaction results in the recruitment of E2F1 to sites of DSBs (10). To determine if UV radiation would also induce an interaction between E2F1 and TopBP1, a co-immunoprecipitation experiment was performed on endogenous E2F1 and TopBP1 proteins. Although a low level of association was observed in untreated cells, UV treatment resulted in an obvious increase in the ability of E2F1 to co-immunoprecipitate TopBP1 (Fig. 3*E*). This suggests that, as with DSBs, binding to TopBP1 may be the mechanism by which E2F1 accumulates at sites of UV-induced DNA damage.

E2F1 Deficiency Impairs the Recruitment of NER Factors to Sites of UV Damage—To determine if E2F1 status affected the recruitment of NER factors to sites of DNA damage, NHFs were transfected with siRNA directed to E2F1 and used in the local UV assay. Depletion of E2F1 did not appreciably

affect the expression levels of several NER factors, including DDB1, DDB2/XPE, XPC, p62 (a component of TFIIH), XPF, XPA, and RPA2 (Fig. 4*A*). However, E2F1 depletion significantly reduced co-localization of XPC, XPA, and p62 with UV damage (Fig. 4, *B–E*). It was previously shown that XPC is required for the recruitment of all other NER factors to sites of UV damage (17). Thus, these findings suggest that E2F1 acts

E2F1 Directly Enhances NER

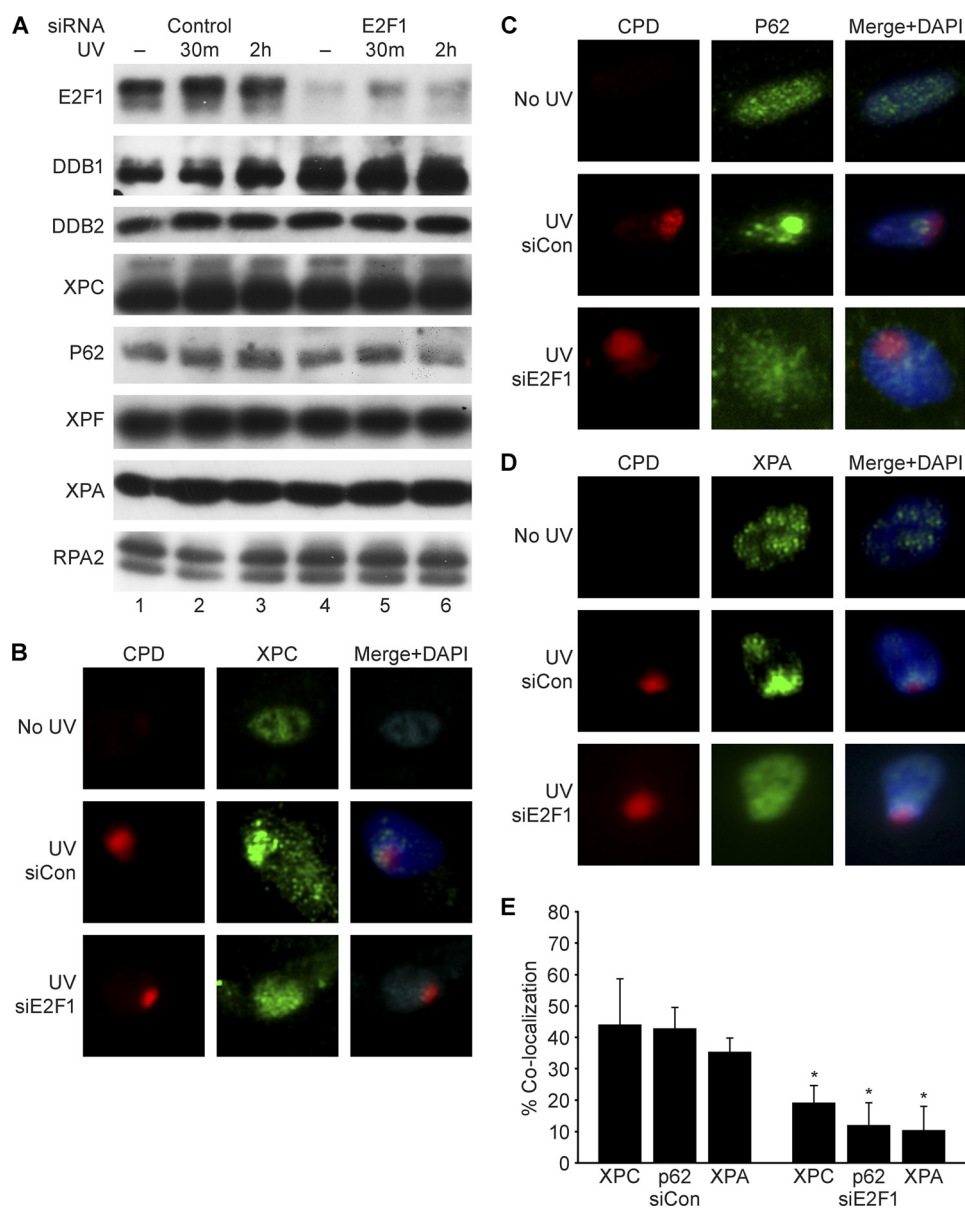


FIGURE 4. E2F1 deficiency impairs the recruitment of NER factors to sites of UV damage. *A*, NHFs were transfected with control siRNA (lanes 1–3) or siRNA specific to E2F1 (lanes 4–6). 24 h later, cells were mock treated (lanes 1 and 4) or exposed to 500 J/m² of UVB and harvested at the indicated time points post-irradiation. Western blot analysis was performed using whole cell lysates and antibodies specific for E2F1 or the DNA repair proteins as indicated. *B–D*, NHFs were mock treated (upper panels) or transfected with control siRNA (siCon, middle panels) or with siRNA to E2F1 (lower panels). Transfected cells were locally irradiated with 50 J/m² of UVC through a filter (middle and lower panels) and 30 min later fluorescently stained for CPD (red) and XPC, XPA, or p62 (green). Cells were counterstained with DAPI and digitally recorded as previously described. *E*, co-localization of XPC, XPA, and p62 with CPD shown in *B–D* were scored from three independent experiments. *, statistically significant difference between siCon- and siE2F1-transfected cells ($p < 0.05$).

upstream of XPC in damage recognition and the recruitment of NER factors.

Stimulation of DNA Repair by E2F1 Requires Serine 31 but Not Functional DNA Binding or Transcriptional Activation Domains—To better understand the function of E2F1 in DNA repair in relation to its other known activities, we performed a series of experiments using a panel of FLAG-tagged E2F1 expression constructs (Fig. 5A). In addition to the S31A mutation, a deletion in the DP dimerization domain also caused defective co-localization of E2F1 with sites of UV

damage (Fig. 5B and supplemental Fig. S1). On the other hand, E2F1 mutants in the DNA binding (E138), Marked box ($\Delta 283$ –358), and C-terminal transactivation ($\Delta 375$ –437) domains were as efficient as wild-type E2F1 in their abilities to accumulate at sites of UV damage. Thus, direct binding to DNA and interactions with protein partners through the Marked box or C terminus is not required for E2F1 to localize to sites of damage. Dimerization with a DP partner may be important for damage localization, although it is also possible that the $\Delta 206$ –220 deletion affects another function important for the accumulation of E2F1 at sites of damage.

To test the ability of these E2F1 mutants to rescue efficient NER, we first knocked down endogenous E2F1 in HCT116 cells by siRNA directed against the 3'-untranslated region region, which is not retained in the exogenous E2F1 expression constructs. As expected, endogenous E2F1 was efficiently knocked down, whereas the exogenously expressed FLAG-E2F1 was not (supplemental Fig. S2A). Plasmids expressing the different FLAG-E2F1 constructs were then transfected back into the cells (Fig. 5C). Because different E2F1 mutant constructs were expressed at different levels, perhaps due to differences in protein stability, the amount of transfected plasmid encoding different mutants was adjusted. Even so, it was difficult to obtain equal expression levels of the various E2F1 constructs. However, it should be pointed out that all E2F1 constructs were expressed at levels above that of endogenous E2F1 (supplemental Fig. S2A, data not

shown). Consistent with our previous findings, the S31A and dimerization domain ($\Delta 206$ –220) mutants did not rescue the impaired co-localization of XPA with CPD caused by depletion of endogenous E2F1. Although the E2F1 $\Delta 283$ –358 mutant localized to sites of damage, it also did not rescue the XPA co-localization defect. In sharp contrast, E2F1 mutants in the DNA binding and transactivation domains promoted the recruitment of XPA to sites of damage to the same degree as wild type E2F1 (Fig. 5D and supplemental Fig. S2B).

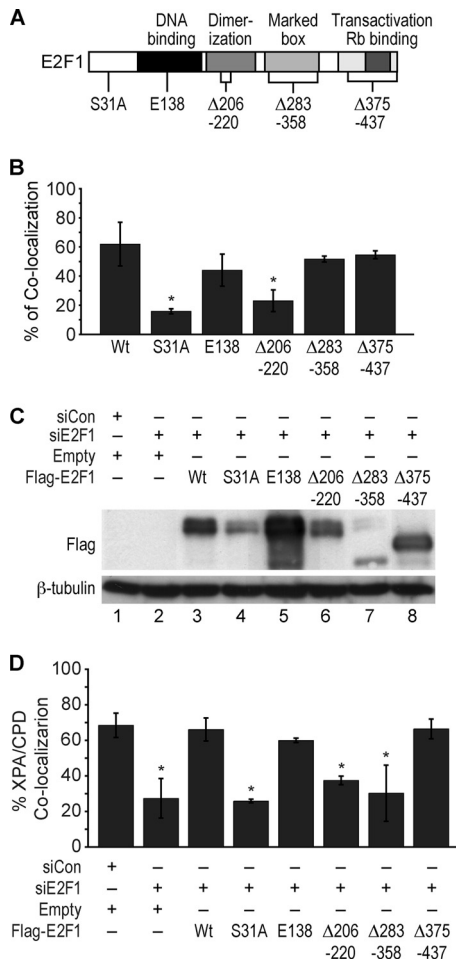


FIGURE 5. Mapping E2F1 domains required for E2F1 and XPA localization to sites of DNA damage. *A*, schematic diagram of E2F1 indicating sites of mutations. *B*, HCT116 cells were transiently transfected with either empty vector or the indicated versions of FLAG-tagged E2F1. Cells were then irradiated with 50 J/m² of UVC through a filter and fluorescently stained for FLAG (green) and CPD (red) 15 min later. Cells were counterstained with DAPI. Co-localization of FLAG tag with CPD were scored as described. The average of two independent experiments is presented. *, statistically significant difference from wild type ($p < 0.05$). *C*, HCT116 cells were co-transfected with control siRNA (siCon, lane 1) or E2F1 siRNA specific to the 3'-untranslated region (lanes 2–8) and empty vector (lane 2) or plasmids expressing wild-type (lane 3) or different mutant versions of FLAG-tagged E2F1 as indicated. 24 h post transfection, Western blot analysis was performed for FLAG tag (top panel) and β-tubulin (bottom panel). *D*, HCT116 cells were transfected as in *C*. Following transfection, cells were exposed to 50 J/m² of UVC through a filter and fluorescently stained for XPA (green) and CPD (red) 15 min post-irradiation. Cells were counterstained with DAPI. Rescue of XPA co-localization with CPD was scored as described. The average of two independent experiments is presented. *, statistically significant difference from cells co-transfected with siCon and empty vector ($p < 0.05$).

Previously we demonstrated that *E2f1* inactivation in mouse cells impaired GG-NER of both (6–4)PP and CPD, although the effect on CPD repair was modest, because this type of lesion is inefficiently repaired in mouse cells. To verify that E2F1 deficiency would inhibit GG-NER in human cells, NHFs were transfected with control or E2F1 siRNA, treated with UV, and the removal of photoproducts from genomic DNA was analyzed by slot blot. As expected, knock down of E2F1 impaired the repair of both (6–4)PP and CPD (Fig. 6A).

To examine the ability of the E2F1 mutants to stimulate GG-NER, HCT116 cells were knocked down for endogenous

E2F1 and transfected with FLAG-E2F1 constructs as described above. Cells were then exposed to UV and harvested immediately (0 h) or at 6 and 24 h post-irradiation. Genomic DNA was then slot-blotted, and antibody specific for the (6–4)PP was used to estimate the amount of DNA damage in each sample. After quantification of band intensities and normalization with total single-stranded DNA, the percentage of photoproduct removal at 6 and 24 h post-irradiation was calculated (Fig. 6B). Ectopic expression of wild-type E2F1 enhanced the removal of (6–4)PP to a rate that was even faster than mock transfected cells. Consistent with the findings above, the S31A, dimerization domain, and Marked box mutants were unable to stimulate GG-NER, whereas E2F1 mutants in the DNA binding and transactivation domains stimulated the removal of DNA damage as efficiently as wild-type E2F1 (Fig. 6B). Given that the DNA binding and transactivation domain mutants are defective for E2F1-mediated transcriptional activation (24), these results strongly suggest that E2F1 enhances GG-NER in a transcription-independent manner.

DISCUSSION

We previously demonstrated that the absence of E2F1 results in inefficient repair of UV-induced DNA damage while E2F1 overexpression stimulates GG-NER (13). This may explain how E2F1, which is normally thought of as a pro-apoptotic factor, functions to inhibit apoptosis and increase survival in response to UV radiation (13, 14). E2F1 has been implicated in regulating the transcription of several genes encoding DNA repair activities, including DDB2/XPE and XPC (25–27). It has been suggested that increased expression of these E2F targets is responsible for the increased NER capacity of cells lacking the retinoblastoma protein (25, 27, 28). However, in normal cells containing the retinoblastoma protein, UV treatment results in the transcriptional repression of E2F target genes, at least during the first 10 h after exposure, when E2F1 status has a significant effect on NER (13, 21, 25, 29). Moreover, we found that E2F1 depletion had no observable effect on the expression levels of DDB2, XPC, or several other NER factors. Instead, our finding that E2F1 accumulates at sites of UV damage and promotes the recruitment of NER factors suggests that E2F1 plays a direct role in GG-NER independent of its ability to regulate transcription. The fact that E2F1 domains critical for activating transcription, namely the DNA binding and transactivation domains, are dispensable for stimulating GG-NER strongly supports a non-transcriptional role for E2F1 in DNA repair.

The ability of E2F1 to stimulate GG-NER requires serine 31, a site phosphorylated by ATR in response to UV irradiation (7). ATR activation occurs when it is recruited to single-stranded DNA coated with replication protein A through an interaction between the ATR dimerization partner ATR-interacting protein and replication protein A (4). ATR kinase activity is then stimulated through a direct physical interaction with TopBP1, which is independently recruited to sites of damage through an association with Rad9 of the 9-1-1 complex (5, 6, 30–32). This process likely initiates at replication or transcription forks stalled by DNA lesions and may require additional processing

E2F1 Directly Enhances NER

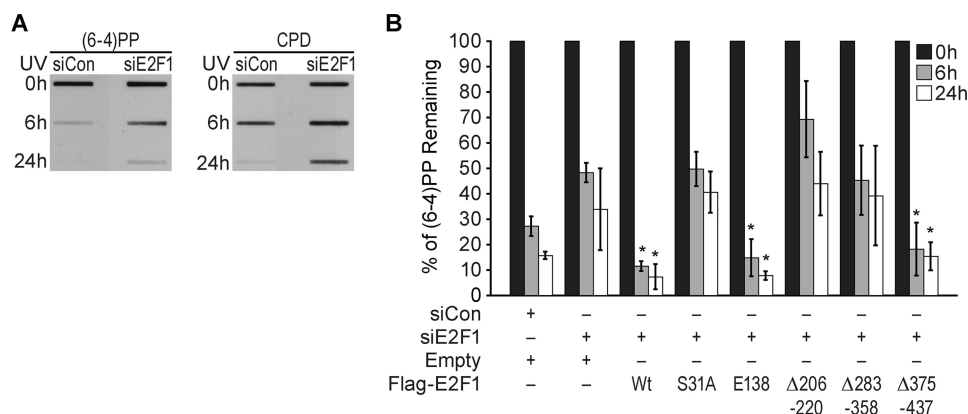


FIGURE 6. Stimulation of GG-NER by E2F1 requires serine 31 but not functional DNA binding or transcriptional activation domains. A, NHEKs were transfected with control siRNA or siRNA to *E2F1* and 24 h later exposed to 500 J/m² of UVB. Genomic DNA (0.5 μg) was taken immediately after UVB treatment (0 h) or 6 and 24 h post-irradiation and slot blotted. DNA damage was detected using antibodies specific for (6-4)PP or CPD. B, HCT116 cells were transfected as described in Fig. 5C. Cells were exposed to 500 J/m² UVB and harvested immediately (0 h) or 6 and 24 h post-irradiation. Genomic DNA was extracted and immuno-slot-blot analysis was performed for (6-4)PP. The intensity of the bands was quantified by ImageJ software, and the results are plotted after normalization with total single strand DNA levels. The average from three independent experiments is presented. *, statistically significant difference from cells transfected with siE2F1 and rescued with empty vector ($p < 0.05$).

by the NER machinery (2, 33–35). We propose that ATR activation then results in the phosphorylation of E2F1 at serine 31, which stabilizes the interaction between E2F1 and TopBP1 at sites of damage. E2F1 then appears to be involved in a process that enhances damage recognition and NER globally throughout the genome.

Several possibilities exist for how E2F1 might enhance damage recognition and GG-NER independent of transcription. It has been demonstrated that E2F1 physically associates with the DDB2/XPE protein (36). In the context of transcription, DDB2/XPE binding stimulates the transcriptional activity of E2F1 (36). Although the effect of E2F1 on DDB2/XPE-mediated repair activity has not been addressed, it is possible that E2F1 association could enhance the damage recognition function of DDB2/XPE. A caveat to this potential mechanism is that DDB2/XPE was shown to bind the C terminus of E2F1, which we found is dispensable for the stimulation of NER by E2F1. Another possibility is that E2F1 indirectly promotes the recruitment of NER factors by recruiting histone-modifying enzymes and altering chromatin structure at sites of damage. This mechanism would be analogous to the mechanism used by E2F1 to stimulate transcription. Future experiments will be aimed at identifying the protein partners that work with E2F1 at sites of damage to facilitate DNA repair.

ATR function has primarily been studied in the context of cell cycle checkpoint signaling, but our previous studies did not find a cell cycle checkpoint defect in response to UV in cells lacking E2F1 (13). Instead, E2F1 may be added to the growing list of ATR targets directly involved in NER, including XPA and XPC (37–39). A recent study suggests that ATR promotes GG-NER only during the S phase, where GG-NER was reported to be less efficient than in other cell cycle phases (40). In contrast, other studies have demonstrated that the cell cycle phase has no impact on NER efficiency (41, 42). Nonetheless, it may be of interest to determine if the E2F1-dependent effect on GG-NER is cell cycle-regulated.

E2F1 can promote or suppress tumor development depending on the experimental context (43). The ability of E2F1 to transcriptionally activate genes important for cell proliferation is thought to be responsible for the oncogenic capacity of E2F1. On the other hand, the molecular mechanism by which E2F1 inhibits tumorigenesis remains unclear. Although it was originally assumed that the ability of E2F1 to induce apoptosis was responsible for this activity, more recent experiments demonstrate no correlation between the regulation of apoptosis and tumor suppression by E2F1 (44). The finding that E2F1 stimulates efficient GG-NER and potentially other forms of DNA repair provides another plausible mechanism by which E2F1 could suppress tumor development.

provides another plausible mechanism by which E2F1 could suppress tumor development.

Acknowledgments—We thank Pam Blau and Jen Smith for technical assistance, Kevin Lin for statistical analysis, Chris Brown for assistance with figures, and Shawnda Sanders and Becky Brooks for preparation of the manuscript. We also thank Karen Vazquez, Rick Wood, Snow Shen, Mark Bedford, Sharon Dent, and Lei Li for helpful comments.

REFERENCES

- Friedberg, E. C. (2001) *Nat. Rev. Cancer* **1**, 22–33
- Lindsey-Boltz, L. A., and Sancar, A. (2007) *Proc. Natl. Acad. Sci. U.S.A.* **104**, 13213–13214
- Hanasoge, S., and Ljungman, M. (2007) *Carcinogenesis* **28**, 2298–2304
- Zou, L., and Elledge, S. J. (2003) *Science* **300**, 1542–1548
- Delacroix, S., Wagner, J. M., Kobayashi, M., Yamamoto, K., and Karnitz, L. M. (2007) *Genes Dev.* **21**, 1472–1477
- Lee, J., Kumagai, A., and Dunphy, W. G. (2007) *J. Biol. Chem.* **282**, 28036–28044
- Lin, W. C., Lin, F. T., and Nevins, J. R. (2001) *Genes Dev.* **15**, 1833–1844
- DeGregori, J., and Johnson, D. G. (2006) *Curr. Mol. Med.* **6**, 739–748
- Wang, B., Liu, K., Lin, F. T., and Lin, W. C. (2004) *J. Biol. Chem.* **279**, 54140–54152
- Liu, K., Lin, F. T., Ruppert, J. M., and Lin, W. C. (2003) *Mol. Cell Biol.* **23**, 3287–3304
- Ianari, A., Natale, T., Calo, E., Ferretti, E., Alesse, E., Screpanti, I., Haigis, K., Gulino, A., and Lees, J. A. (2009) *Cancer Cell* **15**, 184–194
- Pediconi, N., Ianari, A., Costanzo, A., Belloni, L., Gallo, R., Cimino, L., Porcellini, A., Screpanti, I., Balsano, C., Alesse, E., Gulino, A., and Levrero, M. (2003) *Nat. Cell Biol.* **5**, 552–558
- Berton, T. R., Mitchell, D. L., Guo, R., and Johnson, D. G. (2005) *Oncogene* **24**, 2449–2460
- Wikonkal, N. M., Remenyik, E., Knezevic, D., Zhang, W., Liu, M., Zhao, H., Berton, T. R., Johnson, D. G., and Brash, D. E. (2003) *Nat. Cell Biol.* **5**, 655–660
- Moné, M. J., Volker, M., Nikaido, O., Mullenders, L. H., van Zeeland, A. A., Verschure, P. J., Manders, E. M., and van Driel, R. (2001) *EMBO Rep.* **2**, 1013–1017
- Katsumi, S., Kobayashi, N., Imoto, K., Nakagawa, A., Yamashina, Y., Muramatsu, T., Shirai, T., Miyagawa, S., Sugiura, S., Hanaoka, F., Matsunaga,

- T., Nikaido, O., and Mori, T. (2001) *J. Invest. Dermatol.* **117**, 1156–1161
17. Volker, M., Moné, M. J., Karmakar, P., van Hoffen, A., Schul, W., Vermeulen, W., Hoesjmakers, J. H., van Driel, R., van Zeeland, A. A., and Mullenders, L. H. (2001) *Mol. Cell* **8**, 213–224
 18. Fousteri, M., Vermeulen, W., van Zeeland, A. A., and Mullenders, L. H. (2006) *Mol. Cell* **23**, 471–482
 19. Wani, A. A., D'Ambrosio, S. M., and Alvi, N. K. (1987) *Photochem. Photobiol.* **46**, 477–482
 20. Blattner, C., Sparks, A., and Lane, D. (1999) *Mol. Cell Biol.* **19**, 3704–3713
 21. O'Connor, D. J., and Lu, X. (2000) *Oncogene* **19**, 2369–2376
 22. Höfferer, M., Wirbelauer, C., Humar, B., and Krek, W. (1999) *Nucleic Acids Res.* **27**, 491–495
 23. Liu, K., Luo, Y., Lin, F. T., and Lin, W. C. (2004) *Genes Dev.* **18**, 673–686
 24. Cress, W. D., Johnson, D. G., and Nevins, J. R. (1993) *Mol. Cell Biol.* **13**, 6314–6325
 25. Lin, P. S., McPherson, L. A., Chen, A. Y., Sage, J., and Ford, J. M. (2009) *DNA Repair* **8**, 795–802
 26. Polager, S., Kalma, Y., Berkovich, E., and Ginsberg, D. (2002) *Oncogene* **21**, 437–446
 27. Prost, S., Lu, P., Caldwell, H., and Harrison, D. (2007) *Oncogene* **26**, 3572–3581
 28. Bosco, E. E., and Knudsen, E. S. (2005) *Nucleic Acids Res.* **33**, 1581–1592
 29. Yoshida, K., and Inoue, I. (2004) *Oncogene* **23**, 6250–6260
 30. Greer, D. A., Besley, B. D., Kennedy, K. B., and Davey, S. (2003) *Cancer Res.* **63**, 4829–4835
 31. Kumagai, A., Lee, J., Yoo, H. Y., and Dunphy, W. G. (2006) *Cell* **124**, 943–955
 32. Mordes, D. A., Glick, G. G., Zhao, R., and Cortez, D. (2008) *Genes Dev.* **22**, 1478–1489
 33. Marini, F., Nardo, T., Giannattasio, M., Minuzzo, M., Stefanini, M., Plevani, P., and Muzi Falconi, M. (2006) *Proc. Natl. Acad. Sci. U.S.A.* **103**, 17325–17330
 34. O'Driscoll, M., Ruiz-Perez, V. L., Woods, C. G., Jeggo, P. A., and Goodship, J. A. (2003) *Nat. Genet.* **33**, 497–501
 35. Stiff, T., Cerosaletti, K., Concannon, P., O'Driscoll, M., and Jeggo, P. A. (2008) *Hum. Mol. Genet.* **17**, 3247–3253
 36. Hayes, S., Shiyonov, P., Chen, X., and Raychaudhuri, P. (1998) *Mol. Cell Biol.* **18**, 240–249
 37. Matsuoka, S., Ballif, B. A., Smogorzewska, A., McDonald, E. R., 3rd, Hurov, K. E., Luo, J., Bakalarski, C. E., Zhao, Z., Solimini, N., Lerenthal, Y., Shiloh, Y., Gygi, S. P., and Elledge, S. J. (2007) *Science* **316**, 1160–1166
 38. Shell, S. M., Li, Z., Shkriabai, N., Kvaratskhelia, M., Brosey, C., Serrano, M. A., Chazin, W. J., Musich, P. R., and Zou, Y. (2009) *J. Biol. Chem.* **284**, 24213–24222
 39. Wu, X., Shell, S. M., Yang, Z., and Zou, Y. (2006) *Cancer Res.* **66**, 2997–3005
 40. Auclair, Y., Rouget, R., Affar el, B., and Drobetsky, E. A. (2008) *Proc. Natl. Acad. Sci. U.S.A.* **105**, 17896–17901
 41. Mitchell, D. L., Cleaver, J. E., Lowery, M. P., and Hewitt, R. R. (1995) *Mutat. Res.* **337**, 161–167
 42. Wang, Y. C., Maher, V. M., Mitchell, D. L., and McCormick, J. J. (1993) *Mol. Cell Biol.* **13**, 4276–4283
 43. Johnson, D. G., and Degregori, J. (2006) *Curr. Mol. Med.* **6**, 731–738
 44. Rounbehler, R. J., Rogers, P. M., Conti, C. J., and Johnson, D. G. (2002) *Cancer Res.* **62**, 3276–3281